Cantilever dynamics in quasinoncontact force microscopy: Spectroscopic aspects

B. Anczykowski, D. Krüger, and H. Fuchs
Physikalisches Institut, Universität Münster, D-48149 Münster, Germany
(Received 27 July 1995)

The high-amplitude dynamic response of cantilever structures as used in scanning force microscopy was investigated as a function of the probe-sample distance. A computer simulation using the Muller-Yushchenko-Derjaguin/Burgess-Hughes-White (MYD/BHW) method applying realistic surface potentials including adhesion was done. The simulation providing dynamic force-distance curves allows us to attribute discontinuities observed in experimental amplitude-distance curves as the transition points from the purely attractive regime to the repulsive interaction near the lower inflection point of the vibrating probe. [S0163-1829(96)03123-2]

Conventional static force spectroscopy,[1,2] using scanning force microscopes SFM, is based on recording the deflection of a cantilever as a function of the tip-sample distance, as the tip approaches and retracts from a sample surface. This method implies the assumption of a quasistatic displacement of the cantilever, due to interaction forces between a tip and a surface. In contrast, the dynamic SFM mode works with an external periodic force that is applied to the probe and causes the cantilever to oscillate at an adjustable amplitude and frequency. In the quasinoncontact mode, large amplitudes are used (>10 nm), such that the tip propagates virtually all the way through the attractive and partly through the repulsive regime of the surface potential, denoted by V. Therefore, an effective spring constant,

$$k_{\mathrm{eff}}(z)=k+\frac{d^2V}{dz^2}, \tag{1}$$

as given by first-order perturbation theory, as well as linearized models[3] can no longer be applied to investigate this behavior. (The spring constant of the free cantilever is given by k.)

A direct motivation to apply dynamic modes of force microscopy and spectroscopy arises from the field of interfacial phenomena of adhesive surfaces where, for example, contact mode imaging and static force spectroscopy cannot be applied.[4] Rather, approaches based on *true noncontact*[5] and quasinoncontact (''*tapping*'') modes[6] are required to investigate this type of surfaces and to investigate adhesive phenomena locally.

To analyze the dynamic behavior of a cantilever/surface system at high cantilever amplitudes, damping curves can be recorded reflecting the dynamic interaction of the tip with the surface. These curves are a direct measure of the average amplitude of the cantilever oscillation as dependent on the relative tip-sample distance and the driving frequency. Each measurement consists of one complete approach/retraction cycle of the z piezoactuator. The scheme in Fig. 1 shows a characteristic dynamic high-amplitude-distance curve[7] for a complete approach/rectraction cycle of the probe. In addition to the characteristic s-shape behavior of the amplitude-distance curves shown in Fig. 1, small steps and hysteresis loops are measured at distinct distances (denoted as z_0 and z_1 in Fig. 2), indicating a specific change in the tip-sample interaction at the respective probe positions. To investigate the origin of these phenomena, a computer simulation of the approach/retraction process was done.

In the computer simulation of these curves, both repulsive and attractive forces between the probe and the sample surface were considered. Silicon wafers [with (100) oriented surfaces] were used as reference samples both for the experiments and the simulations. The experiments were mainly done in air, using a NanoScope III Dimension 3000 instrument (Digital Instruments). Some experiments were done in a protective gas atmosphere, e.g., dry nitrogen. The silicon wafers were cleaned in a heated ultrasonic cleaner with Milli-Q-grade water and a detergent. The simulations were based on pure silicon surfaces, neglecting the influence of contaminants, such as water and hydrocarbons which are al-

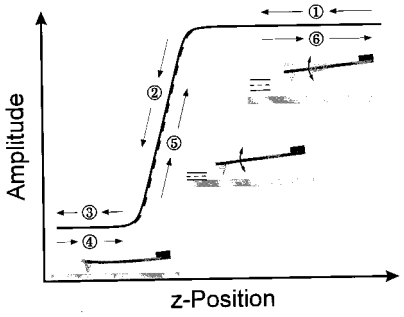

FIG. 1. Scheme of a high-amplitude versus distance curve. Arrows pointing to the left indicate the approach, arrows pointing to the right indicate the retraction movement of the probe to and from the surface, respectively. Positions 1 and 6 characterize the situation of the free oscillating cantilever far away from the surface, with negligible attractive and repulsive forces. At this stage, the (free) oscillation is only damped by the intrinsic shear forces of the cantilever and mainly by its frictional resistance in air (partly also by acoustic effects, i.e., hydrodynamic damping). At positions 2 and 5, interaction forces modify the resonance conditions of the cantilever. The oscillation is then damped and the amplitude decreases linearly with z until a saturation appears. At the left side of the damping curve (positions 3 and 4), the cantilever is sufficiently close to the surface, such that the tip can no longer vibrate. Any further approach of the probe results in a pure static bending of the cantilever. The process is reversible on hard and nonadhesive surfaces such as Si surfaces.

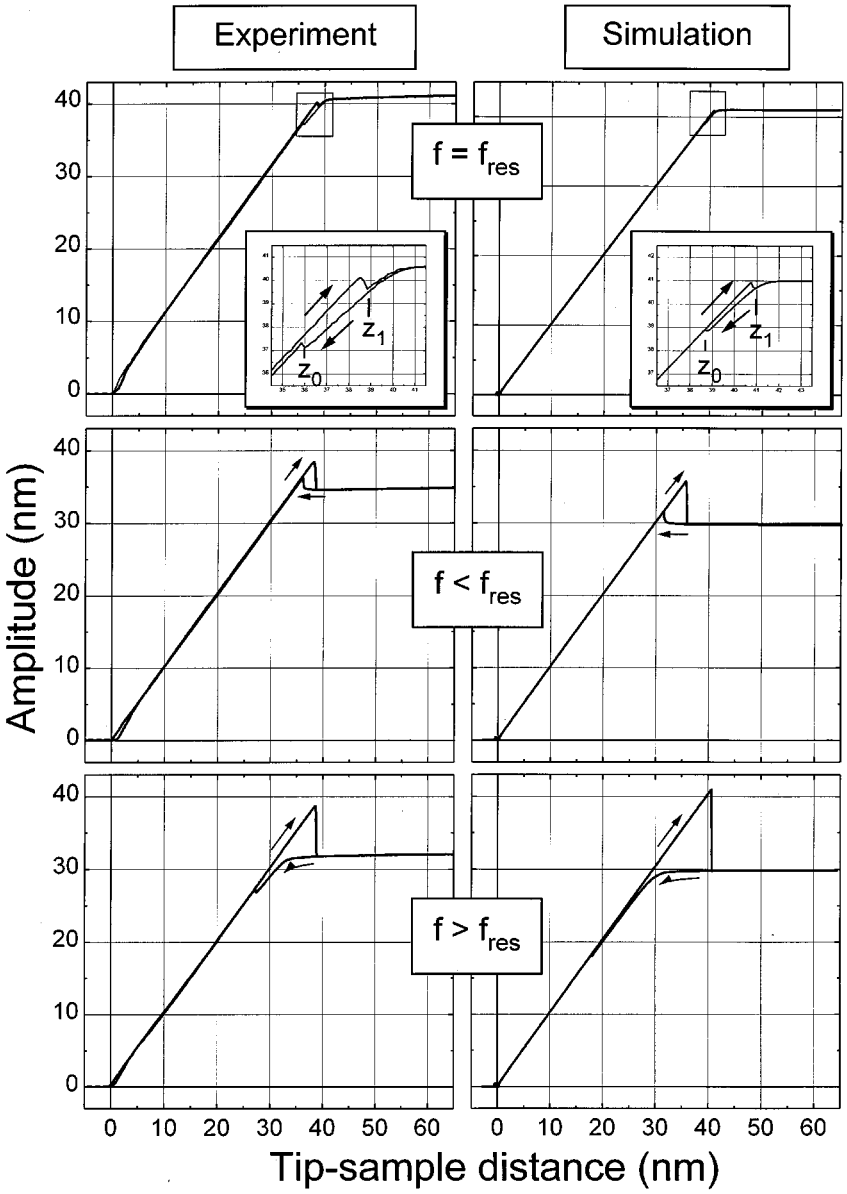

FIG. 2. Experimental amplitude versus distance curves (left column) and computer simulated curves (right column) for high amplitude dynamic force microscopy. The simulation makes use of the Verlet algorithm and the MYD/BHW approximation to model the tip-surface contact (tip radius: 40 nm). (a) SFM cantilever driven in resonance; (b) cantilever driven below; and (c) above resonance. Computational time for a single trace consisting of 512 sample points: 1.5 h on a Pentium CPU. Experimental acquisition time per trace: 2.5 s.

ways present in experiments done in air. Thus, by comparing experimental results and computer simulations, the influence of contaminants in high amplitude dynamic force microscopy on real samples can be studied. To estimate the spring constants of the Si cantilevers used (Nanoprobe), scanning electron microscopy images (Leica Stereoscan 440) were used to determine their geometric properties. Other key parameters, such as the resonance frequency f_{res}, the resonance amplitude A_{res}, and the quality factor Q, required for the simulation of the dynamic system, were derived from the resonance curve of each individual cantilever used for the experiments.

The cantilever dynamics can be described by the differential equation:

$$m\ddot{z}+\alpha\dot{z}+kz+F(z)=F_0\sin\omega t, \tag{2}$$

where α denotes the damping constant; F_0 and ω are the amplitude and the frequency of the driving force, respectively. $F(z)$ is the force acting between tip and surface at the relative distance z. Equation (2) implies two assumptions: First, α is supposed to be independent of z. Assuming a small elastic sample deformation in the repulsive regime, as induced by the probing tip, this should be an appropriate approximation as the hydrodynamic damping is then dominating the friction term α. As for the distance regime considered here (<50 nm), the change in hydrodynamic damping is negligible,[8] α may be set constant. Second, the elastic relaxation time of the materials should be small compared with the time the tip indents the sample. This allows us to consider a force between tip and sample that depends only on the relative distance z.

Typical amplitudes of cantilever oscillations in the quasinoncontact (tapping) mode are in the range of 10–100 nm. Typical widths of surface potentials are significantly smaller. The tip will, therefore, move through large parts of the attractive and repulsive regimes of the surface potential during each oscillation cycle. Consequently, the dynamic behavior of the tip cannot be correctly described by a linearized potential[9] anymore, or by considering pure harmonic potentials by introducing different (static) cantilever spring con-

stants for the free cantilever and the repulsive tip/surface contact.[10] However, using a more realistic force-distance dependence $F(z)$, Eq. (2) cannot be integrated analytically. On the other hand, a more general approach as used here allows us to include both elastic deformations and attractive (e.g., adhesive) forces. Discrete values of $F(z)$ can be calculated numerically with the MYD/BHW model[11,12] (using a sphere/plate geometry here), while the whole $F(z)$ dependence can then be approximated with a cubic spline.

The integration of the equation of motion [Eq. (2)] can then be done by using the Verlet algorithm:[13]

$$z(t+\Delta t)=2z(t)-z(t-\Delta t)+\Delta t^2\ddot{z}(t), \tag{3}$$

with the velocity obtained by the central difference,

$$\dot{z}=\frac{z(t+\Delta t)-z(t-\Delta t)}{2\Delta t}. \tag{4}$$

With Eq. (2), this results in

$$z(t+\Delta t)=C_1\{C_2z(t)+C_3z(t-\Delta t) + C_4[F\sin\omega t-F(z(t))]\}, \tag{5}$$

with the following coefficients: $C_1=[1+\Delta t\alpha/(2m)]^{-1}$; $C_2=2-\Delta t^2k/m$; $C_3=\Delta t\alpha/(2m)-1$; $C_4=\Delta t^2m$. The time steps Δt used in the simulation should be small compared with the sampling period time T (the simulations presented here were calculated with $\Delta t=T/1000$). The damping curves can be simulated with this method by approaching the surface at a constant speed v and averaging the oscillation amplitudes. The curves obtained in this way can be directly compared with the experimental results.

In addition, the computer simulation provides information about the forces exerted on the sample as dependent on z. The calculated average forces $F(z_{\min})$ at the lower inflection point $z_{\min}$ can be recorded at every distance of the probe and reflect both the extreme value of the forces and the nature of the operation mode, i.e., true noncontact $[F(z_{\min})<0]$ or tapping $[F(z_{\min})>0]$ mode.

The dynamic measurements and the computer simulations were done for three different cases (Fig. 2). To compare experimental findings and computer results driving frequencies exactly at, below, and above the resonance frequency, f_{res} of the free cantilever were chosen. For the system constants k, α, m, and F_0 that are required to perform the simulation using Eq. (5), the following independent system parameters were applied: $k=42.1$ N/m, $Q=492$, $f_{\text{res}}=311.5$ kHz, $A_{\text{res}}=41$ nm.

As shown in Fig. 2, the computer simulation and the experimental results agree well for the three frequency regimes investigated. On approaching the tip to the surface while driving the cantilever in resonance [Fig. 2(a)], the oscillation amplitude will first slowly *decrease*. Closer to the surface the amplitude decreases linearly with the sample distance over a short distance. At a distinct distance z_0, a discontinuity appears [see inset of Fig. 2(a)], such that the amplitude abruptly increases and the damping curve is shifted towards a slightly higher amplitude. On retracting the tip, another discontinuity occurs at a larger distance $z_1>z_0$, where the amplitude reaches its original value. As a result, a hysteresis of the amplitude versus distance curve is observed. This reflects the bistable behavior of a resonator in a nonlinear potential.[14]

By driving the cantilever below its resonance frequency [Fig. 2(b)], the amplitude first *increases* on approaching the sample. Below this point, both approach and retraction curves are identical. Retracting the cantilever results in a linear increase above the amplitude of the free oscillation, until the amplitude suddenly falls back to the original value at z_1. In the computer simulation [Fig. 2(b), right], this increase reaches about 90% of the amplitude of free oscillation in resonance, the maximum amplitude of the system.

Using a driving frequency above resonance [Fig. 2(c)], the ''approaching'' amplitudes show a similar dependence as in the resonance case. The main difference is that the discontinuity appears at a distance z_0, which is closer to the surface. In the simulation, this point is almost at zero distance, such that the hysteresis appears over the whole decreasing part of the curve. The retracting curve exhibits the same characteristic shape as that shown in Fig. 2(b): the oscillation amplitude increases above that of the free oscillation before it reaches its original value at z_1.

The observed steplike discontinuity in the linearly decreasing regime of the damping curves cannot be readily understood from the experimental amplitude-distance data alone. Rather, this can be done with the computer simulation, which allows us not only to analyze the amplitude of the cantilever oscillation at a given distance z, but also provides the corresponding *dynamic force-distance curves* (Fig. 3). In particular, the average forces calculated at the lower inflection points of the cantilevers, as obtained by the simulation, allow us to explain the experimental damping curves. In the resonance case [Fig. 3(a)], the forces first appear to be purely attractive while approaching the surface. The step occurring in the (approaching) damping curve at z_0 [see Fig. 2(a)] is related to the onset of the repulsive regime of the surface potential, i.e., the oscillation switches from a purely noncontact oscillation (pure attractive interaction) to the tapping mode (attractive and repulsive), as seen in Fig. 3(a). On retracting the cantilever the oscillation remains in this quasinoncontact mode until the second step appears at the large distance of z_1.

The forces acting on the tip with the cantilever driven below resonance [Fig. 3(b)] indicate that the oscillation is in the quasinoncontact (tapping) mode at virtually every distance z to the surface once the tip has reached the attractive regime of the surface potential. At the beginning of the tip approach, the oscillation amplitude *increases* [see Fig. 2(b)]. This effect can be explained by a decrease of the effective spring constant, due to the attractive interaction potential. As a consequence, the resonance frequency of the cantilever decreases, resulting in a shift of its resonance curve to lower eigenfrequencies. This causes the observed increase in the oscillation amplitude. In this case, the pure attractive dynamic SFM mode cannot be adjusted, as the size of the resonance enhanced cantilever amplitude becomes comparable with the tip/sample distance. As a consequence, the quasinoncontact (''tapping'') mode occurs automatically, i.e., independently of the distance z. This results in an increase of the force exerted on the sample, due to the repulsive interaction involved.

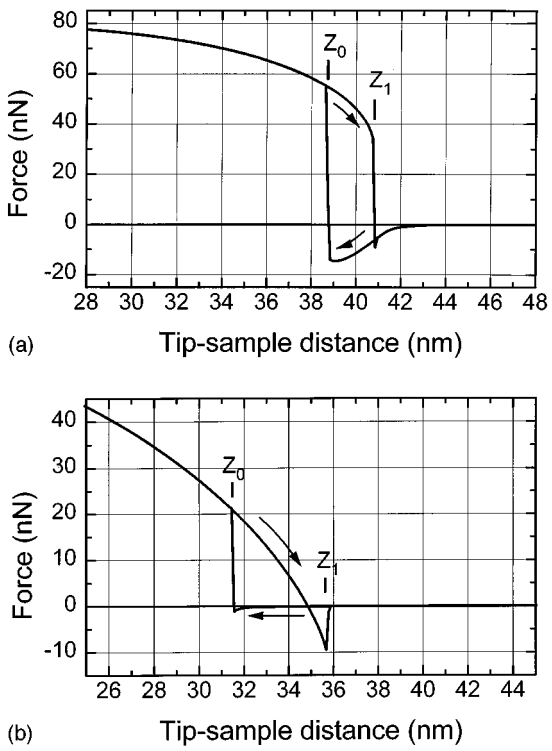

FIG. 3. (a) Calculated force-distance curve for the resonance case. The force curve clearly indicates the onset of a steep repulsive force at the distance z_0, where the step is observed in the amplitude damping curve during approach [see Fig. 2(a)]. On retraction, the force stays repulsive (quasinoncontact) until the second step in the damping curve is reached at z_1. (b) Calculated force-distance curve with the driving frequency set below the eigenresonance of the free cantilever [see Fig. 2(b)]. In contrast to (a), the tip switches almost immediately to the repulsive regime at z_0 (see text). A pronounced attractive force is only obtained during retraction of the cantilever near z_1. (Arrows as in Fig. 1.)

To summarize, the computer simulations presented lead to a more detailed understanding of the experimental approach curves in high amplitude-dynamic force microscopy. The results provide quantitative parameters necessary for obtaining images in the pure noncontact dynamic mode, even at very high oscillation amplitudes. The simulation shows, that while setting the driving frequency above or at resonance, forces will be minimized when probing in the attractive regime. On the other hand, these settings will cause higher forces compared to a cantilever driven below resonance, as soon as the oscillation switches to the quasinoncontact mode. The simulation also shows that the feedback control may become unstable with these settings as soon as the first discontinuity in the damping curve is reached at z_0 on approaching the probe. Then, due to the bistable behavior of the cantilever, two distinct amplitude values become possible with the distance z decreasing. As expected, forces excerted on the sample will strongly increases when the oscillation switches to the quasinoncontact mode from the pure attractive regime.

The computer simulations also demonstrate that the cantilever dynamic behavior, using high amplitudes, is very sensitive to the surface potential applied. Especially, when applying linearized models, and models applying purely harmonic surface potentials and Hertzian mechanics, the numerical results deviate sizeably from the experimental findings.[15] This also justifies the more general numerical approach discussed here, making use of the MYD/BHW model. Within this approach, only a small qualitative difference between the simulations (pure conditions) and the experiments done in air were observed. No significant difference was observed when a dry nitrogen atmosphere was applied instead of (humid) air. While the different step heights of the hysteresis loops in experiment and simulation might be partly attributed to the influence of contamination layers, the widths of the simulated hysteresis loops (z_1-z_0) were found to be dependent on the effective tip radius.[15] In conclusion, by combining dynamic SFM with methods used in molecular dynamics as done here, an approach for dynamic force spectroscopy (DFS) is obtained. This opens different perspectives, for example, for obtaining a better understanding of strongly attractive interactions, such as adhesive phenomena on the nanometer scale.

We thank L. F. Chi, M. Neizert, and R. Ellerbrake for their help and discussions.

[1] N. A. Burnham and R. J. Colton, in *Force Microscopy*, edited by D. A. Bonnell (VCH Publishers, Inc., New York, 1990), Chap. 7, pp. 191–249.

[2] D. Sarid, *Scanning Force Microscopy With Applications to Electric, Magnetic, and Atomic Forces*, Oxford Series on Optical Sciences (Oxford University Press, New York, 1991).

[3] M. Nonnenmacher, Ph.D. thesis, University of Kassel, Kassel, 1990.

[4] B. Anczykowski, L. F. Chi, and H. Fuchs, Surf. Interface Anal. **23**, 416 (1995).

[5] Y. Martin, C. C. Williams, and H. K. Wickramasinghe, J. Appl. Phys. **61**, 4723 (1987).

[6] Q. Zhong, D. Imniss, K. Kjoller, and V. B. Elings, Surf. Sci. **290**, L688 (1993).

[7] J. Chen, R. K. Workman, D. Sarid, and Ralf Höper, Nanotechnology **5**, 199 (1994).

[8] P. Güthner, Ph.D. thesis, University of Konstanz, Konstanz, 1992.

[9] U. Düring, O. Züger, and A. Stalder, J. Appl. Phys. **72**, 1778 (1992).

[10] J. P. Spatz, S. Sheiko, M. Moller, R. G. Winkler, P. Reineker, and O. Marti, Nanotechnology **6**, 40 (1995).

[11] V. M. Muller, V. S. Yushenko, and B. V. Derjaguin, J. Colloid Interface Sci. **77**, 91 (1980).

[12] B. D. Hughes and L. R. White, J. Mech. Appl. Math. **32**, 445 (1979).

[13] L. Verlet, Phys. Rev. **159**, 98 (1967).

[14] P. Gleyzes, P. K. Kuo, and A. C. Boccarra, Appl. Phys. Lett. **58**, 2989 (1991).

[15] B. Anczykowski, D. Krüger, and H. Fuchs (unpublished).